Journal of Organometallic Chemistry 889 (2019) 9–14

Contents lists available at ScienceDirect

Journal of Organometallic Chemistry

journal homepage: www.elsevier.com/locate/jorganchem

DFT study of inter-ring haptotropic rearrangement in $CpRu^+$ complexes of polycyclic aromatic ligands

Igor P. Gloriozov [a], Mikhail S. Nechaev [a, b], Kirill V. Zaitsev [a, *], Yuri F. Oprunenko [a, **], Franck Gam [c], Jean-Yves Saillard [c, ***]

[a] Department of Chemistry, M.V. Lomonosov Moscow State University, Leninskie Gory, 119991, Moscow, Russia
[b] A. V. Topchiev Institute of Petrochemical Synthesis, Russian Academy of Sciences, Leninsky Prospect 29, 119991, Moscow, Russia
[c] Univ. Rennes, CNRS, ISCR-UMR 6226, F-35000, Rennes, France[1]

ARTICLE INFO

Article history:
Received 24 January 2019
Received in revised form
20 March 2019
Accepted 21 March 2019
Available online 26 March 2019

Keywords:
Ruthenium complexes of polyaromatics
Inter-ring haptotropic rearrangement
Organometallic complexes of graphene
DFT calculations

ABSTRACT

Inter-ring haptotropic rearrangements (IRHRs) of different types are well-known phenomena in organometallic and catalytic chemistry. So far, they are reported for transition metal complexes with carbo- and heterocyclic polyaromatic hydrocarbons (PAH) of small and medium size. Here, we report DFT studies of $RuCp^+$ shifts between neighboring six-membered rings ($\eta^6 \rightleftharpoons \eta^6$-IRHR) on an extra-large PAH as a model for graphene and compare it to naphthalene. Our calculations predict that $\eta^6 \rightleftharpoons \eta^6$-IRHRs proceed with much lower activation energy barrier of rearrangement in the case of the $RuCp^+$ complex of η^6-graphene model.

1. Introduction

Transition metal complexes play a decisive role in the transformation of simple organic substances and generation of important innovative derivatives such as technological precursors, materials for science and industry, catalysts, new polymers and medicines [1]. In the case of complexes of polyaromatic hydrocarbons (PAHs), these properties are generally associated with their structural peculiarities and propensity for inter-ring rearrangements (IRHRs) both via dissociative inter- and intra-molecular mechanism [2]. They consist in the shifting of an ML_n organometallic group (OMG) along the PAH plane from one ring to another. Such $\eta^n \rightleftharpoons \eta^n$-IRHR (n = 2, Ni, Rh; n = 4, Ir; n = 6, Cr, Ru) were observed for a number of transition metals, and in particular investigated for chromium tricarbonyl complexes [3]. Some examples involving naphthalene complexes are shown in Scheme 1.

So far only a very restricted number of $\eta^6 \rightleftharpoons \eta^6$-IRHRs in $RuCp^+$ complexes of PAH, which are quite important as catalysts [4] and as antitumor agents [5], were reliably observed (Scheme 2). Thus, such rearrangements were reported in complexes of acecorannulene [6] and rubrene [7]. The activation barriers were estimated as $\Delta G^{\#}$ ~25–30 kcal/mol. Dynamic behavior of transition metal complexes is quite important, in particular in the course of transformations of ruthenium complexes, due to the fact that during IRHR via transition states and intermediates, the hapticity of the metal decreases. As a consequence, it can catch in its coordination sphere additional substrate and reagent for the act of catalysis [8]. Low activation barrier facilitates shifting of the metal at reasonable temperatures and catalytic reaction in much milder conditions. Large PAH such as graphene and nanotubes have anticancer activity themselves [9] and proved activity of $RuCp^+$ complexes [10] can leads to increasing activity in synergetic mode after coordination with ruthenium.

Though these two reactions are difficult to compare, owing to the considerable differences of the PAH structures, both with rigid stereochemistry of the ligands (bowl-type geometry of acecorannulene and propeller-like conformation of periphery phenyls in rubrene). Additionally Cp^* is a more donor ligand than Cp, and this also differentiates both complexes. But overall, this is the nature of

* Corresponding author.
** Corresponding author.
*** Corresponding author.
E-mail addresses: zaitsev@org.chem.msu.ru (K.V. Zaitsev), oprunenko@org.chem.msu.ru, oprunenko@mail.ru (Y.F. Oprunenko), jean-yves.saillard@univ-rennes1.fr (J.-Y. Saillard).
URL: http://fhmas.ru/ru/personal_oprunenko.htm
[1] http://www.scienceschimiques.univ-rennes1.fr/equipes/cti/.

https://doi.org/10.1016/j.jorganchem.2019.03.016
0022-328X/

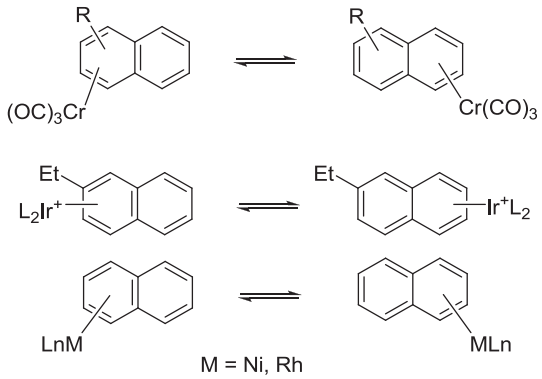

Scheme 1. Examples of inter-ring rearrangements (IRHRs) for naphthalene complexes.

the ion pairs which is the main factor facilitating IRHR. In non-polar solvents such as CH_2Cl_2, contact ion pairs (CIPs) are formed between Ru^+ and the counter-ion (e.g. PF_6^-). Such ion pairing facilitates the IRHR process, in contrast to what happens in polar solvents where separated ion pairs (SIPs) are formed [11]. Indeed, $\eta^6 \rightleftharpoons \eta^6$-IRHR is sufficiently rapid (hours) in CH_2Cl_2 solvent, and extremely slow (weeks) in the much more polar acetone solvent. This means that IRHR activation barriers in ruthenium cationic complexes depend on cation–anion and cation–solvent interactions [12]. This agrees well with the fact that for more than two decades it has been well-known that reaction rates of the majority of processes in organometallic $CpRu^+$ salts depend on the solvent and the structure of ion pairs [13]. Later, we have shown by DFT calculations that, in the case of non-polar solvents, interaction of negative counter ion (e.g. PF_6^-) with (η^6-naphthalene)$RuCp^+$ via the metal in CIP can considerably reduce activation barriers thus making $\eta^6 \rightleftharpoons \eta^6$-IRHR possible at reasonable temperature. The problem of experimental kinetic measurement of such barriers by means of *e.g.* spectroscopic methods consists in the poor weak complex concentration, due to low solubility of such salts in non-polar solvents [11].

Except for the two processes illustrated in Scheme 2, a quite exotic *electron-driven* haptotropic reaction was observed recently [14] in a complex containing both Ru and Fe metal centers (Scheme 3). The reaction was initiated by oxidation of Fe^0 into Fe^+ in the initial complex. Thus, this redox electronic factor owing to partial positive charge in the substituent decrease electron density in substituted ring and considerably reduces the activation barrier and thus allows the $\mathbf{A^{2+}} \rightleftharpoons \mathbf{B^{2+}}$ IRHR.

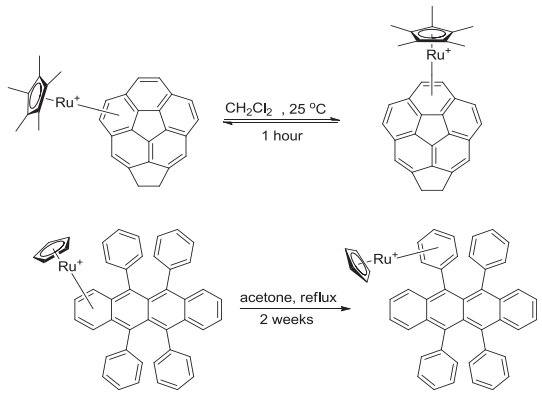

Scheme 2. Examples of inter-ring rearrangements (IRHRs) for $RuCp^+$ complexes of polyaromatic hydrocarbons (PAHs).

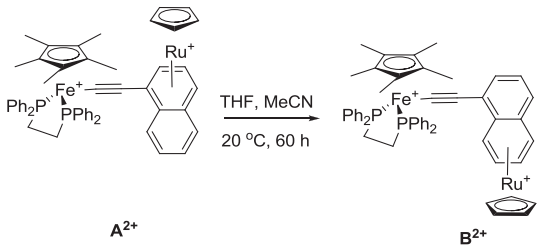

Scheme 3. *Electron-driven* haptotropic reaction.

Another possibility to reduce considerably the activation barrier for an (η^6-arene)$RuCp^+$ species was demonstrated in the case of naphthalene complexes substituted with highly donor Si-groups (Scheme 4) [15]. The mechanism involves *contact* of the coordinating solvent molecule with Ru^+, which facilitates the **C** ⇌ **D** rearrangements. This was observed experimentally and supported theoretically by DFT ($\Delta G^{\#}$~30 kcal/mol) for a number of $RuCp^+$ complexes [16]. It is noteworthy that the $\eta^6 \rightleftharpoons \eta^6$-IRHR proceeds from the donor-substituted ring to the unsubstituted naphthalene ring which has considerably less electron density, supporting thus the idea that the bonding of coordinating MeCN solvent molecules with Ru^+ is the driving force of the IRHR. Full or partial electron charge delocalization (*e.g.* from counter-anion) on the ligand also plays a considerable role in reducing the IRHR activation barrier, as it was founded by *McGlinchey* et al. [17–19]. It is however quite difficult to separate this contribution from DFT calculations in the case of polycyclic aromatic ligand, the structure of which consists of uncharged six-membered rings.

Finally, it should be noted that IRHR processes can be also accelerated with the use of UV/vis irradiation, as demonstrated by *Perekalin* et al. [16] in the case of substituted naphthalene complexes (Scheme 5) for which the rearrangement is much faster than when thermally induced even at low temperature after deprotonating of the corresponding acid in water.

For the sake of comparison we have calculated the activation barrier for such UV-induced process in the case of the unsubstituted (η^6-naphthalene)$RuCp^+$ assuming SIP state. The IRHR reaction takes place in the exited low-lying triplet state and requires a fairly low activation barrier ($\Delta G^{\#} = 13.4$ kcal/mol). These calculations were in part published in a diploma work [20], they are provided here in more details in the SI. These results prove the applicability of DFT for the calculation of activation barrier of IRHR.

In contrast, recent experimental investigations of $\eta^6 \rightleftharpoons \eta^6$-IRHRs in synthesized Cp^*Ru^+ complexes of a number of common PAH showed the absence of any rearrangement, in polar solvents [21]. This was supported by DFT calculations which led to very high activation barriers ($\Delta G^{\#} = 36–41$ kcal/mol), precluding observation of such rearrangements at reasonable temperatures. These results are in accordance with our systematic DFT investigation of $\eta^6 \rightleftharpoons \eta^6$-IRHR in ($\eta^6$-naphthalene)$MCp^+$ (M = Fe, Ru, Os) complexes as solvent SIP [20], which also show very high activation barrier $\Delta G^{\#} = 40–47$ kcal/mol (see Fig. S3 and Table S1, Supplementary).

The analysis of the above data strongly suggests that the only

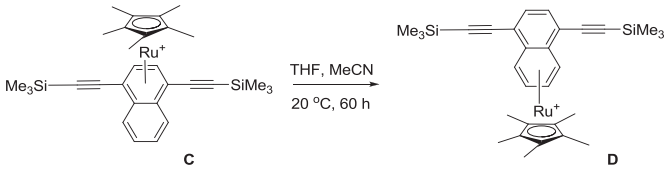

Scheme 4. Rearrangement for silicon substituted Ru complex.

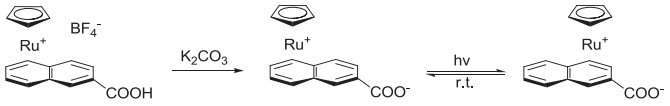

Scheme 5. Rearrangement for Ru complex under UV/vis irradiation.

possibility to observe thermally driven IRHR at reliable temperatures in *small* and *middle* size PAH (except for introducing strong electron donating/withdrawing substituent) is to include as a catalyst some efficient *coordinating agent* which in the course of reaction can bind to Ru^+. Alternatively, one could proceeds the reaction in a very dilute solution (which strongly complicates spectroscopic observation) in *non-polar* solvents to preserve CIP formation with the counter ion coordinated to Ru^+. Experiments to find such universal conditions for $\eta^6 \rightleftharpoons \eta^6$-IRHRs in $CpRu^+$ complexes are now in progress. The results could be of high importance in catalysis and material science.

But to our mind another possibility also exists to facilitate $\eta^6 \rightleftharpoons \eta^6$-IRHRs in $RuCp^+$ complexes, not considered in the literature before. It consists in increasing the size of the PAH because in that case the metal-PAH bonding is weaker, allowing an easier metal migration along the PAH surface. This was already proven for tricarbonyls of group 6 metals (M = Cr, Mo, W) with large coronene and kekulene [22], as well as graphene [23] and nanotubes [24]. This trend was supported by *Sato* et al. [25] with the result of some decrease of activation barrier for (η^6-coronene)$RuCp^+$ ($\Delta G^{\#} = 31–33$ kcal/mol) in comparison with the data on IRHR for small PAH ($\Delta G^{\#} = 36–41$ kcal/mol) [21]. In this paper, we further increase the size of the PAH model by two additional layers around the central coronene molecule, thus modeling already non-synthesized $RuCp^+$ complexes of graphene with the ($C_{96}H_{24}$) $RuCp^+$ complex **I** and we show by DFT calculations that the computed IRHR energy barriers are much lower than with complexes of smaller PAHs.

2. Results and discussion

There are six types of symmetry-equivalent rings in the considered $C_{96}H_{24}$ PAH for coordination with $CpRu^+$. We discuss herein the only models where the metal is coordinated to the two most inner rings (**I-A** and **I-B**; see Fig. 1), because it was shown previously that activation barriers depend poorly on localization of the metal on the sheet of the model graphene ligand [23]. They are also more representative of coordination to extended graphene systems. Their small energy difference (~2 kcal/mol, see Fig. 1) indicates that our chosen model graphene is pertinent. In the course of $\eta^6 \rightleftharpoons \eta^6$-IRHR in **I-A**, where the metal is situated at the very center of the model "graphene" molecule, the $RuCp^+$ unit shifts via transition state **I-TS1**, intermediate **I-IM** and second transition state **I-TS2** to the neighboring ring with the formation of the complex **I-B**, where $CpRu^+$ has practically same configuration as in **I-A**: **I-A** $\rightleftharpoons$ **I-TS1** $\rightleftharpoons$ **I-IM** $\rightleftharpoons$ **I-TS2** $\rightleftharpoons$ **I-B**. The intermediate and the two transition states have very similar structures and are very close in energy (Fig. 1). Noteworthy, the activation barrier is considerably reduced ($\Delta G^{\#} = 25.5$ kcal/mol) relative to small and middle size PAH ($\Delta G^{\#} \sim 36–41$ kcal/mol).

Such a lowering of the activation barrier for the sliding of $RuCp^+$ along the PAH is consistent with a considerable Ru-C bond length increase in **I-A** (or **I-B**), in comparison with that in the η^6-naphthalene ruthenium complex **II** (Figs. 1 and 2 and Table 1). In model **I**, $RuCp^+$ will continue to shift to the periphery due to thermodynamic preferences along the surface of the ligand. However, considering that a graphene flake has only a restricted perimeter in comparison with the huge amount of inner six-membered rings in pristine graphene means that movement of $RuCp^+$ will occur mainly in the middle of graphene and thus process **I-A** $\rightleftharpoons$ **I-B** is most characteristic for $RuCp^+$ complexes IRHR in graphene.

In order to get a deeper insight in the bonding variation within the stationary points of **I**, a Morokuma-Ziegler energy decomposition analysis (EDA) was carried out, considering the interaction between the PAH and $RuCp^+$ fragments (see Computational Details). For the sake of comparison, a similar analysis was performed for **II**. The results are given in Table 2, where the total bonding energy between fragments is expressed as the sum of three components, the Pauli repulsion (E_{Pauli}), the electrostatic interaction energy (E_{Elstat}), and the orbital interaction energy (E_{orb}). Unsurprisingly, the Pauli repulsion decreases with metal connectivity. It is overbalanced by the stabilizing E_{Elstat} and E_{orb} components, of which E_{orb} is prevailing, indicating covalency predominance. The total bonding energy is lower in **II-A** as compared with **I-A** (or **I-B**), confirming stronger bonding with smaller PAH. Consistently, a population analysis of the fragment frontier orbitals in **I-A** and **II-A** indicates that the electron transfers corresponding to PAH → metal donation and metal → PAH backdonation are larger in **II-A** than in **I-A** (0.61 *vs.* 0.51 and 1.08 *vs.* 0.98, respectively). On the other hand, the opposite energetic situation occurs for the reaction intermediates, *i.e.*, the bonding is stronger in the graphene system **I-IM**. This is in line with the much larger electron delocalization in the larger PAH. This can be also related to the different natures of the IRHR processes in **I** (inner) and **II** (outer), as illustrated in Figs. 1 and 2. As a result, in **I-IM** Ru is η^4-coordinated, somewhat like in a trimethylenemethane complex, but with three long bonds (2.50–2.52 Å) and a short one (2.12 Å), whereas **II-IM** is in a peripheral η^3 coordination mode (see Figs. 1 and 2 and Table 1). The population analysis of the fragment frontier orbitals indicates a substantially larger PAH → metal electron transfer in **I-IM** (0.98) than in **II-IM** (0.62). Although much less pronounced, the difference in the metal → PAH backdonation follows the same trend (0.37 in **I-IM** *vs.* 0.30 in **II-IM**). As a consequence of a more stable **A** equilibrium geometry and a less stable intermediate **IM** (or the very close transition states) in the case of **I** as compared to **II**, their energy difference is smaller in the graphene complex **I** than in its naphthalene relative **II** and so is the activation energy in the $\eta^6 \rightleftharpoons \eta^6$-IRHR process.

Thus, from the obtained results we can draw a conclusion that for η^6-$RuCp^+$ complexes of sufficiently large PAH (graphene, nanotubes, fullerenes) thermally induced $\eta^6 \rightleftharpoons \eta^6$-IRHR with high rate at reliable temperature (50–70 °C) is possible. Moreover, owing to the significantly smaller HOMO-LUMO gap of **I** as compared to **II** (Figs. S1 and S2), one may anticipate that the UV–vis induced process should be even much faster in the case of large PAH.

3. Computational details

The geometries of molecules, transition states, and intermediates were fully optimized by means of density functional theory (DFT) calculations. The PBE functional [26] and scalar-relativistic theory were used, the latter employing the four-component spin-free Hamiltonian derived by *Dyall* [27] and applied variationally [28]. The full electron basis sets L1 were used, where L1 stands for double set size. The numbers of contracted and primitive functions used in L1 are respectively {2,1}/{6,2} for H, {3,2,1}/{10,7,3} for C, and {7,6,4}/{26,23,16,5} for Ru [29]. Such functionals and basis sets were chosen as the result of a systematic investigation of the geometry of various metal complexes and the rates of organometallic reactions which was accomplished in our laboratory during the past decade as well as a result of comparative calculations in the course of this work. Corrections for zero-point

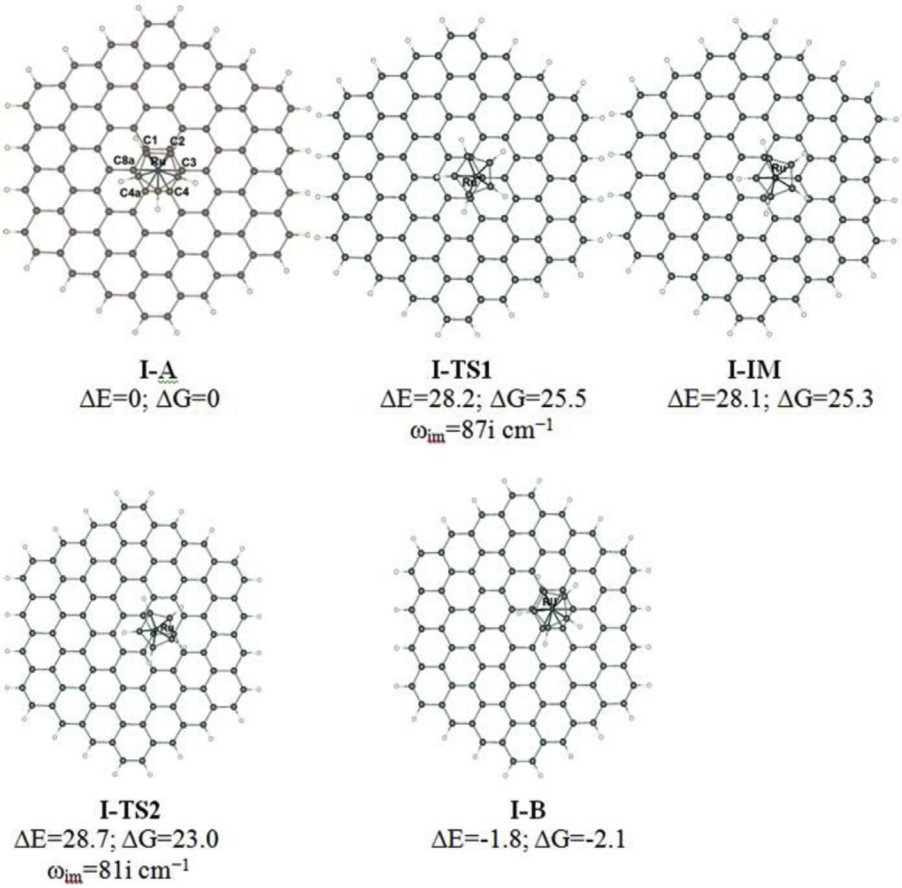

Fig. 1. Structures and energies (in kcal mol^{-1}) of the stationary points along the $\eta^6 \rightleftharpoons \eta^6$-IRHR pathway in η^6-grapheneRuCp$^+$ (**I**), numeration in Cp fragment omitted for the sake of simplicity and is the same as in Fig. 2 for **II-A**.

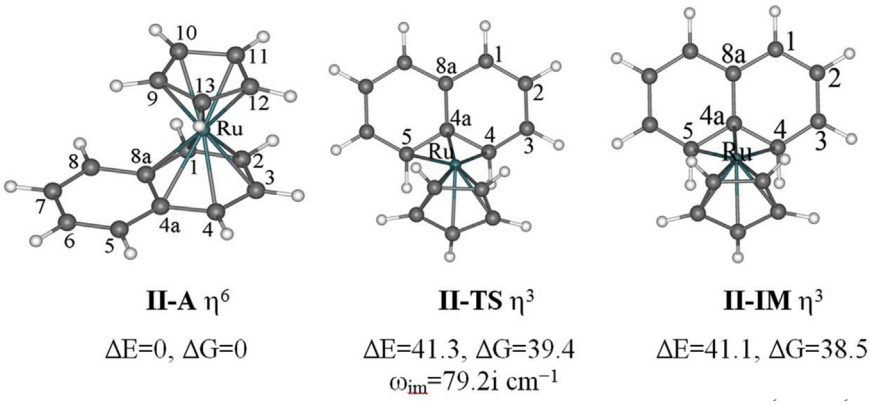

Fig. 2. Structures and energies (in kcal/mol) of the stationary points along the $\eta^6 \rightleftharpoons \eta^6$-IRHR pathway in ($\eta^6$-naphthalene)RuCp$^+$ (**II**). Owing to the pathway symmetry, only its first half is considered.

energies were calculated in the harmonic approximation. Stationary points on the potential energy surface (PES) were identified by analyzing Hessians. The thermodynamic functions (Gibbs activation energies, G) at 298.15 K were calculated using an approximation of restricted rotator and harmonic oscillator. Reaction paths were found by the intrinsic reaction coordinate (IRC) method. All calculations were performed using the MBC100k cluster at the Joint Supercomputer Center (JSCC) (Moscow, Russia) with the use of the PRIRODA04 program written by *Laikov* [29,30].

The interactions between the PAH and RuCp$^+$ fragments were investigated within the Morokuma-Ziegler energy decomposition analysis (EDA) framework [31,32]. Whereas, PRIRODA04 does not provide such EDA analysis, we used the ADF program [33,34], carrying out single-point calculations on the PRIRODA04-optimized structures, employing the PBE functional, and using the standard TZ2P basis set within the zeroth-order regular approximation (ZORA) [35]. It was checked that both programs provide no significant differences in terms of relative energies. It was also

Table 1
Selected bond lengths in **II** [20] and **I** (in Å).

Bond	X-ray **II-A**	DFT **II-A**	DFT **I-A**
Ru-C1	2.218	2.216	2.303
Ru-C2	2.221	2.224	2.303
Ru-C3	2.218	2.225	2.303
Ru-C4	2.200	2.218	2.302
Ru-C4a	2.284	2.310	2.302
Ru-C8a	2.262	2.309	2.303
Ru-C9	2.179	2.214	2.178
Ru-C10	2.190	2.207	2.178
Ru-C11	2.182	2.184	2.178
Ru-C12	2.172	2.182	2.178
Ru-C13	2.180	2.203	2.178
C4a-C8a	1.441	1.453	1.437
C2-C3	1.422	1.424	1.437
C6-C7	1.428	1.425	1.427
Average deviation for X-ray and DFT for **II-A**	–	0.015	

Table 2
Morokuma-Ziegler energy decomposition analysis (EDA) of **I** and **II** (all values in eV). E_{Pauli} = Pauli repulsion; E_{elstat} = electrostatic interaction; E_{Orb} = orbital interaction. TBE = (total bonding energy) = $E_{Pauli} + E_{elstat} + E_{orb}$.

	I-A	**I-TS1**	**I-IM**	**I-TS2**	**I-B**	**II-A**	**II-IM**
E_{Pauli}	7.16	5.14	5.55	4.98	7.33	8.42	5.02
E_{Elstat}	−4.39	−3.45	−3.69	−3.34	−4.49	−5.26	−3.42
E_{Orb}	−6.63	−4.22	−4.41	−4.13	−6.79	−7.31	−3.85
TBE	−3.86	−2.53	−2.55	−2.49	−3.95	−4.15	−2.25

checked by test calculations with a hybrid functional (PBE0 [36]) that the discussed results are stable with respect to the functional nature (see Table S2).

4. Conclusions

By means of DFT $\eta^6 \rightleftharpoons \eta^6$-IRHR, their mechanisms and relative energies of intermediates and transition states in $RuCp^+$ complexes of naphthalene and of a model graphene molecule $C_{96}H_{24}$ (**I**) were investigated and analyzed. Theoretical data are in good agreement with quantitative experimental kinetic data for other PAH complexes. The metal shift on the graphene ligand proceeds through two transition states and one intermediate. Increasing the PAH size leads to a considerable reduction of the activation barrier of the thermally induced $\eta^6 \rightleftharpoons \eta^6$-IRHR and thus facilitates migration of the $RuCp^+$ in comparison with small and middle-sized PAH.

Acknowledgments

The authors thank Alexander von Humboldt Stiftung (Bonn, Germany) for providing the workstation and some other software accessories to perform DFT calculations. Part of this work was done by Nechaev M.S. in the frame of TIPS RAS State Plan. F. G. thanks the Région Bretagne for a PhD studentship (ARED NANOCLU 9334).

Appendix A. Supplementary data

Supplementary data to this article can be found online at https://doi.org/10.1016/j.jorganchem.2019.03.016.

References

[1] a) S.G. Davies, Organotransition Metal Chemistry: Applications to Organic Synthesis, vol. 2, Elsevier, Tetrahedron Organic Chemistry, Amsterdam, Netherlands, 2013;
b) D. Alberico, M.E. Scott, M. Lautens, Aryl–aryl bond formation by transition-metal-catalyzed direct arylation, Chem. Rev. 107 (2007) 174–238.

[2] a) Y.F. Oprunenko, Inter-ring haptotropic rearrangements in π-complexes of transition metals with polycyclic aromatic ligands, Russ. Chem. Rev. 69 (2000) 683–704;
b) I.D. Gridnev, O.L. Tok, in: M. Gielen, R. Willem, B. Wrackmeyer (Eds.), Fluxional Organometallic and Coordination Compound, Wiley, New York, 2004, pp. 41–81.

[3] Y.F. Oprunenko, N.G. Akhmedov, D.N. Laikov, S.G. Malyugina, V.I. Mstislavsky, V.A. Roznyatovsky, N.A. Ustynyuk, Regioselective synthesis of π-complexes of substituted polycyclic aromatic compounds. Experimental (NMR) and theoretical (DFT) studies of η^6,η^6-haptotropic rearrangements in naphthalenechromiumtricarbonyl complexes, J. Organomet. Chem. 583 (1999) 136–145.

[4] E.P. Kündig, Synthesis of transition metal η^6-arene complexes, in: Transition Metal Arene p-Complexes in Organic Synthesis and Catalysis, Springer, Berlin Heidelberg, 2004, pp. 3–20.

[5] a) V. Moreno, J. Lorenzo, F.X. Aviles, M.H. Garcia, J.P. Ribeiro, T.S. Morais, M.P. Robalo, Studies of the antiproliferative activity of ruthenium (II) cyclopentadienyl-derived complexes with nitrogen coordinated ligands, Bioinorgan. Chem. Appl. (2010) 1–12;
b) Y.K. Yan, M. Melchart, A. Habtemariam, P.J. Sadler, Organometallic chemistry, biology and medicine: ruthenium arene anticancer complexes, Chem. Commun. (2005) 4764–4776.

[6] T.J. Seiders, K.K. Baldridge, J.M. O'Connor, J.S. Siegel, Ring selectivity and migratory aptitude of Cp^*Ru^+ complexation to acecorannulene, Chem. Commun. (2004) 950–951.

[7] R.S. Koefod, K.R. Mann, Ring shift isomerization reaction of monocyclopentadienylruthenium (II) complexes of rubrene. Kinetic and thermodynamic studies of metal-arene binding selectivity, J. Am. Chem. Soc. 112 (1990) 7287–7293.

[8] C. Elschenbroich, Organometallics, John Wiley & Sons, 2016.

[9] Z.M. Markovic, L.M. Harhaji-Trajkovic, B.M. Todorovic-Markovic, D.P. Kepić, K.M. Arsikin, S.P. Jovanović, V.S. Trajkovic, In vitro comparison of the photothermal anticancer activity of graphene nanoparticles and carbon nanotubes, Biomaterials 32 (2011), 1221-1129.

[10] Y.K. Yan, M. Melchart, A. Habtemariam, P.J. Sadler, Organometallic chemistry, biology and medicine: ruthenium arene anticancer complexes, Chem. Commun. (2005) 4764–4776.

[11] E.O. Fetisov, I.P. Gloriozov, Y.F. Oprunenko, J.Y. Saillard, S. Kahlal, Influence of ion pairing in inter-ring haptotropic rearrangements in cationic cyclopentadienyl complexes of ruthenium with naphthalene: a DFT investigation, Organometallics 32 (2013) 3512–3520.

[12] R.E. Lehmann, T.M. Bockman, J.K. Kochi, Concurrent one-and two-electron processes in electrophile/nucleophile interactions of organometallic ion pairs, J. Am. Chem. Soc. 112 (1990) 458–459.

[13] A. Moreno, P.S. Pregosin, L.F. Veiros, A. Albinati, S. Rizzato, PGSE NMR diffusion overhauser studies on [Ru (Cp^*)(η^6-arene)][PF_6], plus a variety of transition-metal, inorganic, and organic salts: an overview of ion pairing in dichloromethane, Chem. Eur A J. 14 (2008) 5617–5629.

[14] R. Makhoul, H. Sahnoune, T. Davin, S. Kahlal, V. Dorcet, T. Roisnel, C. Lapinte, Proton-controlled regioselective synthesis of [Cp^*(dppe)Fe–C-C-1-(η^6-$C_{10}H_7$)Ru(η^5-Cp)](PF_6) and electron-driven haptotropic rearrangement of the (η^5-Cp)Ru^+ arenophile, Organometallics 33 (2014) 4792–4802.

[15] R. Makhoul, J.A. Shaw-Taberlet, H. Sahnoune, V. Dorcet, S. Kahlal, J.F. Halet, C. Lapinte, Complexation of the (η^5-Cp)Ru^+ and (η^5-Cp^*)Ru^+ arenophiles on alkynylnaphthalene: solvent effect on the regioselectivity and the haptotropic rearrangement, Organometallics 33 (2014) 6023–6032.

[16] D.S. Perekalin, E.E. Karslyan, P.V. Petrovskii, A.O. Borissova, K.A. Lyssenko, A.R. Kudinov, Arene exchange in the ruthenium–naphthalene complex [$CpRu(C_{10}H_8)]^+$, Eur. J. Inorg. Chem. (2012) 1485–1492.

[17] A. Decken, J.F. Britten, M.J. McGlinchey, Facile haptotropic shifts in organometallic complexes of 4H-cyclopenta[def]phenanthrene via naphthalene-type transition states: synthetic, X-ray crystallographic, NMR spectroscopic, and EHMO studies, J. Am. Chem. Soc. 115 (1993) 7275–7284.

[18] S.S. Rigby, H.K. Gupta, N.H. Werstiuk, A.D. Bain, M.J. McGlinchey, The barriers to trimethylsilyl migrations in indenes and benzindenes: silatropic shifts via aromatic transition states, Polyhedron 14 (1995) 2787–2796.

[19] S.S. Rigby, H.K. Gupta, N.H. Werstiuk, A.D. Bain, M.J. McGlinchey, Do aromatic transition states lower barriers to silatropic shifts? A synthetic, NMR spectroscopic, and computational study, Inorg. Chim. Acta 251 (1996) 355–364.

[20] E.O. Fetisov, DFT Study of $RuCp^+$ Complexes of Polyaromatic Ligands, Diploma Thesis, Department of Chemistry, Moscow State University, Moscow, Russia, 2012 (in Russ.).

[21] M. Rioja, P. Hamon, T. Roisnel, S. Sinbandhit, M. Fuentealba, K. Letelier, J.-Y. Saillard, J.R. Hamon, [(η^5-C_5Me_5)Ru]$^+$ fragments ligated to polyaromatic hydrocarbons: an experimental and computational approach to pathways for haptotropic migration, Dalton Trans. 44 (2015) 316–329.

[22] N.S. Zhulyaev, I.P. Gloriozov, Y.F. Oprunenko, J.-Y. Saillard, DFT study of chromium tricarbonyl complexes of coronene and kekulene, Moscow Univ. Chem. Bull. (Engl. Transl.) 72 (2017) 201–211.

[23] I.P. Gloriozov, R. Marchal, J.-Y. Saillard, Yu. F. Oprunenko, Chromium tricarbonyl and chromium benzene complexes of graphene, their properties, stabilities, and inter-ring haptotropic rearrangements– a DFT investigation, Eur. J. Inorg. Chem. (2015) 250–257.

[24] a) F. Nunzi, F. Mercuri, F. De Angelis, A. Sgamellotti, N. Re, P. Giannozzi, Coordination and haptotropic rearrangement of $Cr(CO)_3$ on (n, 0) nanotube

sidewalls: a dynamical density functional study, J. Phys. Chem. B 108 (2004) 5243–5249;
b) N.S. Zhulayev, DFT Study of 6 Group Metal Complexes of Polyaromatic Ligands from Coronene to Graphene, Diploma Thesis, Department of Chemistry, Moscow State University, Moscow, Russia, 2018 (in Russ.).
[25] H. Sato, C. Kikumori, S. Sakaki, Solvation structure of coronene–transition metal complex: a RISM-SCF study, Phys. Chem. Chem. Phys. 13 (2011) 309–313.
[26] J.P. Perdew, K. Burke, M. Ernzerhof, Generalized gradient approximation made simple, Phys. Rev. Lett. 77 (1996) 3865–3868.
[27] K.G. Dyall, An exact separation of the spin-free and spin-dependent terms of the Dirac–Coulomb–Breit Hamiltonian, J. Chem. Phys. 100 (1994) 2118–2127.
[28] D.N. Laikov, A new class of atomic basis functions for accurate electronic structure calculations of molecules, Chem. Phys. Lett. 416 (2005) 116–120.
[29] D.N. Laikov, Fast evaluation of density functional exchange-correlation terms using the expansion of the electron density in auxiliary basis sets, Chem. Phys. Lett. 281 (1997) 151–156.
[30] D.N. Laikov, Y.A. Ustynyuk, PRIRODA-04: a quantum-chemical program suite. New possibilities in the study of molecular systems with the application of parallel computing, Russ. Chem. Bull. 54 (2005) 820–826.
[31] K. Morokuma, Molecular orbital studies of hydrogen bonds. III. C=O···H–O hydrogen bond in $H_2CO\cdots H_2O$ and $H_2CO\cdots 2H_2O$, J. Chem. Phys. 55 (1971) 1236–1244.
[32] T. Ziegler, A. Rauk, A theoretical study of the ethylene-metal bond in complexes between copper(1+), silver(1+), gold(1+), platinum(0) or platinum(2+) and ethylene, based on the Hartree-Fock-Slater transition-state method, Inorg. Chem. 18 (1979) 1558–1565.
[33] G. te Velde, F.M. Bickelhaupt, S.J.A. van Gisbergen, C. Fonseca Guerra, E.J. Baerends, J.G. Snijders, T. Ziegler, Chemistry with ADF, J. Comput. Chem. 22 (2001) 931–967.
[34] ADF, SCM, Theoretical Chemistry, Vrije Universiteit, Amsterdam, The Netherlands, 2013. http://www.scm.com.
[35] E. van Lenthe, E.-J. Baerends, J.G. Snijders, Relativistic total energy using regular approximations, J. Chem. Phys. 101 (1994) 9783–9792.
[36] C. Adamo, V. Barone, Toward reliable density functional methods without adjustable parameters: the PBE0 model, J. Chem. Phys. 110 (1999) 6158–6169.